

Theoretical Modeling of the High Redshift Galaxy Population

David H. Weinberg

Department of Astronomy, Ohio State University, Columbus, OH 43210

Romeel Davé

Astrophysical Sciences, Princeton University, Princeton, NJ 08544

Jeffrey P. Gardner

Department of Astronomy, University of Washington, Seattle, WA 98195

Lars Hernquist

Department of Astronomy, Harvard University, Cambridge, MA 02138

Neal Katz

Department of Physics and Astronomy, University of Massachusetts, Amherst, MA 98195

Abstract. We review theoretical approaches to the study of galaxy formation, with emphasis on the role of hydrodynamic cosmological simulations in modeling the high redshift galaxy population. We present new predictions for the abundance of star-forming galaxies in the LCDM model (inflation + cold dark matter, with $\Omega_m = 0.4$, $\Omega_\Lambda = 0.6$), combining results from several simulations to probe a wide range of redshift. At a threshold density of one object per arcmin² per unit redshift, these simulations predict galaxies with star formation rates of $2M_\odot/\text{yr}$ ($z = 10$), $5M_\odot/\text{yr}$ ($z = 8$), $20M_\odot/\text{yr}$ ($z = 6$), $70 - 100M_\odot/\text{yr}$ ($z = 4 - 2$), and $30M_\odot/\text{yr}$ ($z = 0.5$). For galaxies selected at a fixed comoving space density $n = 0.003 h^3\text{Mpc}^{-3}$, a simulation of a $50h^{-1}$ Mpc cube predicts a galaxy correlation function $(r/5h^{-1} \text{Mpc})^{-1.8}$ in comoving coordinates, essentially independent of redshift from $z = 4$ to $z = 0.5$. Different cosmological models predict global histories of star formation that reflect their overall histories of mass clustering, but robust numerical predictions of the comoving space density of star formation are difficult because the simulations miss the contribution from galaxies below their resolution limit. The LCDM model appears to predict a star formation history with roughly the shape inferred from observations, but it produces too many stars at low redshift, predicting $\Omega_\star \approx 0.015$ at $z = 0$. We conclude with a brief discussion of this discrepancy and three others that suggest gaps in our current theory of galaxy formation: small disks, steep central halo profiles, and an excess of low mass dark halos. While these problems

could fade as the simulations or observations improve, they could also guide us towards a new understanding of galactic scale star formation, the spectrum of primordial fluctuations, or the nature of dark matter.

1. Theoretical Approaches to Galaxy Formation

In broad outline, the current theory of galaxy formation is remarkably similar to the one described by White & Rees (1978) two decades ago. Gravitational instability of primordial density fluctuations leads to the collapse of dark matter halos. Gas falls into these potential wells, heats up as it does so, then radiates its energy, loses pressure support, contracts, and eventually forms stars. Dissipation thus leads to the formation of dense baryonic cores, which can survive as distinct entities even if their parent dark halos merge.

Relative to the situation in 1978, we now have much better theoretical models for the origin of the primordial fluctuations, with inflation as the leading candidate. There has also been a major change to the theoretical picture, the idea that the dominant mass component is not baryonic dark matter but some form of non-baryonic, cold dark matter (CDM). No existing models that assume purely baryonic matter can account for the cosmic structure seen today while remaining consistent with the observed low amplitude of cosmic microwave background anisotropies. In inflation+CDM models normalized to the COBE observations, the properties of the initial conditions for structure formation are completely determined by a small number of parameters, principally Ω_m , Ω_b , and Ω_Λ (the density parameters of matter, baryons, and vacuum energy), H_0 , and the inflationary spectral index n (where $n = 1$ corresponds to scale-invariant fluctuations).

There have also been substantial developments in the “technology” for modeling galaxy formation theoretically. One line of attack, semi-analytic modeling, descends directly from the approach of White & Rees (1978). These methods use extensions of the Press-Schechter (1974) formalism that describe merger histories of collisionless dark matter halos (Bond et al. 1991, Bower 1991, Lacey & Cole 1994). They adopt an idealized description of gas dynamics and cooling within halos and incorporate parametrized models of star formation from cooling gas and reheating by supernova feedback (e.g., White & Frenk 1991, Kauffmann et al. 1993, Cole et al. 1994, Avila-Reese et al. 1998, Somerville & Primack 1999). A simpler branch of this work focuses on the properties of galaxy disks, with the halo spin parameter playing a critical role (Fall & Efstathiou 1980, Dalcanton et al. 1997, Mo et al. 1998). The semi-analytic approach allows traditional population synthesis and chemical evolution models to be placed in a far more realistic framework of structure formation. There are numerous free parameters to be set either by normalization to observations or by calibration against numerical simulations, but once these parameters are fixed the models can be tested against many independent observations. The strengths of semi-analytic models lie in their ability to make contact with a wide range of observations, their ability to explore a wide range of theoretical parameter space, and their description of galaxy formation in simple and physically intuitive terms. The semi-analytic approach can also be combined with N-body simulations to sidestep some of

the approximations used in the halo merger models and, more importantly, to obtain detailed predictions of galaxy clustering (e.g., Governato et al. 1998, Kauffmann et al. 1999ab).

The other main approach to theoretical modeling of galaxy formation is direct numerical simulation, including hydrodynamics and star formation. There are two broad classes of simulations, those that zoom in on individual objects (e.g., Katz & Gunn 1991, Katz 1992, Navarro & White 1994, Vedel et al. 1994, Steinmetz & Müller 1994, Navarro & Steinmetz 1997, Dominguez-Tenreiro et al. 1998, Kaellender & Hultman 1998) and those that simulate larger, random realizations of cosmological volumes (e.g., Cen & Ostriker 1992, Katz et al. 1992, Evrard et al. 1994, Pearce et al. 1999). The main goal of the first class of simulations is to study the formation mechanisms and properties of individual galaxies, while the main goal of the second is to study spatial clustering of the galaxy population and the statistical distributions of galaxies' stellar, gas, and total masses. There are two main technical approaches, Eulerian grid codes and smoothed particle hydrodynamics (SPH), with Lagrangian grid codes (Gnedin 1995, Pen 1998) having intermediate properties. Eulerian grid codes can often achieve high mass resolution (i.e., have many grid cells and hence small mass per cell), but the uniformity of the fixed grid means that the spatial resolution in computing hydrodynamic forces is usually rather low (though it can be improved by using multiple grids, as in Anninos & Norman [1996]). For example, the recent simulations of Cen & Ostriker (1999) use $200h^{-1}$ kpc grid cells and attempt to identify sites and rates of galactic level star formation based on the gas properties averaged over this scale. SPH simulations compute hydrodynamic forces by smoothing over a fixed number of particles and therefore have higher spatial resolution in denser regions. In SPH simulations that include radiative cooling, the gas in well resolved halos almost invariably has a two-phase structure, with dense, cold lumps embedded in a hot, pressure-supported medium. The cold lumps have sizes and masses roughly comparable to the luminous regions of observed galaxies, and they stand out distinctly from the background, so that there is no ambiguity in identifying the "galaxies" in such simulations.

Relative to semi-analytic modeling of galaxy formation, the strength of the numerical simulation approach is its more realistic treatment of gravitational collapse, mergers, and heating and cooling of gas within dark halos. The difference in treatment could be quantitatively important, since the simulations show that gas and galaxies are distributed along filamentary networks that resemble the root system of a tree, making the accretion process very different from the spherically symmetric one envisaged in the semi-analytic calculations. The only free parameters (apart from the physical parameters of the cosmological model being studied) are those related to the treatment of star formation and feedback. Given these parameters, simulations provide straightforward, untunable predictions. However, the simulation approach must contend with the numerical uncertainties caused by finite volume and finite resolution, and computational expense makes it a slow way to explore parameter space.

2. Numerical Simulations of the High-Redshift Galaxy Population

Our group’s approach to hydrodynamic cosmological simulations is described in detail by Katz et al. (1996). We use a cosmological version of the Hernquist & Katz (1989) TreeSPH code; the results shown here are from simulations that use the parallel code developed by Davé et al. (1997). In brief, the simulations use two sets of particles to represent the dark matter and gas components, respectively. Dark matter particles respond only to gravitational forces, which are computed using a hierarchical tree method (Barnes & Hut 1986). Gas particles respond to gravity and to gas dynamical forces computed by SPH. The simulations include heating by shocks, adiabatic compression, and photoionization, and cooling by adiabatic expansion, Compton interaction with the microwave background, and, most importantly, all of the radiative atomic processes that arise in a primordial composition gas.

In simulations without star formation, a fraction of the gas condenses into cold, dense lumps, with typical sizes of one to several kpc, and masses up to a few $\times 10^{11} M_{\odot}$. Our star formation algorithm is essentially a prescription for turning this cold, dense gas into collisionless stars, returning energy from supernova feedback to the surrounding medium. A gas particle is “eligible” to form stars if it is Jeans unstable, resides in a region of converging flow, and has a physical density exceeding 0.1 hydrogen atoms cm^{-3} . Once a gas particle is *eligible* to form stars, its star formation *rate* is given by

$$\frac{d\rho_{\star}}{dt} = -\frac{d\rho_g}{dt} = \frac{c_{\star}\epsilon_{\star}\rho_g}{t_g}, \quad (1)$$

where $c_{\star} = 0.1$ is a dimensionless star formation rate parameter, $\epsilon_{\star} = 1/3$ is the fraction of the particle’s gas mass that will be converted to stellar mass in a single simulation timestep, and the gas flow timescale t_g is the maximum of the local gas dynamical time and the local cooling time. Recycled gas and supernova feedback energy are distributed to the particle and its neighbors. Because the surrounding medium is dense and has a short cooling time, the feedback energy is usually radiated away rather quickly, so it has only a modest impact in our simulations.

This description of galactic scale star formation is clearly idealized, but our predictions of galaxy properties are not sensitive to its details. As shown in Katz et al. (1996), changing c_{\star} by an order of magnitude makes almost no difference to the stellar masses of simulated galaxies. With lower c_{\star} , gas simply settles to higher density before star formation begins to deplete it, and the dependence of $d\rho_{\star}/dt$ on ρ_g and t_g in equation (1) ensures that star formation cannot get too far out of step with the rate at which gas cools out of the hot halo. One could, however, imagine radically different formulations of galactic scale star formation that would lead to different results, e.g., if cooled gas does not form stars steadily but instead accumulates until an interaction triggers a violent starburst. One could also imagine a picture in which multi-phase substructure in the ISM allows supernova feedback to have a greater impact on the surrounding halo gas.

We have analyzed the clustering of galaxies at $z = 2 - 4$ in simulations of a variety of CDM models in Katz et al. (1999, hereafter KHW), and we will discuss the star formation properties of the galaxies in those simulations

in a forthcoming paper. Here we focus instead on results that cover a wider range of redshifts for a single model: flat cosmology with $\Omega_m = 0.4$, $\Omega_\Lambda = 0.6$, $\Omega_b = 0.0473$, $h = 0.65$, $n = 0.95$, with a COBE-normalized mass fluctuation amplitude $\sigma_8 = 0.80$ on the scale of $8h^{-1}$ Mpc at $z = 0$. We have been carrying out simulations of this LCDM model with a range of box sizes, particle numbers, and ending redshifts, to address a variety of questions, including the influence of numerical parameters on the predictions of high redshift structure.

Figure 1 presents the result most relevant to those searching for high- z galaxies: the predicted surface density of objects as a function of star formation rate (SFR), from $z = 10$ to $z = 0.5$. The SFR can be converted approximately to a UV continuum luminosity using one’s favorite IMF and population synthesis model. For example, the model adopted by Steidel et al. (1996) gives an absolute magnitude $M_{AB} = -20.8$ at rest-frame wavelength 1500\AA for $\text{SFR} = 10M_\odot/\text{yr}$. Each line type in Figure 1 corresponds to a simulation with a different number of particles and/or simulation box size, as indicated by the legends. In general, simulations with higher mass resolution better represent the low end of the luminosity function, while simulations with larger volume better represent the high end. Since limited resolution and limited box size both cause underestimates of galaxy numbers, one can generally take the highest line at a given SFR in a given panel as a lower limit to the predicted surface density of objects. In panels where the curves from different simulations connect up, we can infer that the prediction based on the upper envelope of these curves is reasonably robust to the numerical parameters of the simulations, though of course it may still be sensitive to the cosmological parameters and to the adopted model of star formation.

Table 1. Parameters of the LCDM Simulations

Title	N	R	ϵ_{grav}	$60m_{\text{dark}}$	$60m_{\text{SPH}}$
n128r5	128^3	5.55	1.25	7.4×10^8	9.9×10^7
n128r11	128^3	11.11	2.5	5.9×10^9	7.9×10^8
n64r11	64^3	11.11	5	4.7×10^{10}	6.3×10^9
n144r50	144^3	50.0	10	3.8×10^{11}	5.1×10^{10}

Table 1 lists the parameters of the simulations shown in Figure 1: the number of particles of each species, the size of the simulation cube (in comoving h^{-1} Mpc), the gravitational force softening length (in comoving h^{-1} kpc), and approximate mass resolution limits (in M_\odot). In examination of the simulations, we find that dark halos containing at least 60 dark matter particles essentially always contain a simulated galaxy, and we therefore list $60m_{\text{dark}}$ as a minimum resolved dark halo mass. The requirement for robustly estimating the SFR via equation (1) seems to be somewhat more stringent, 60 or more particles in the dissipated baryon component (*cold* gas + stars), and we therefore list $60m_{\text{SPH}}$ as the minimum baryon mass of a resolved galaxy. The curves in Figure 1 are computed only for galaxies above this resolution limit, and the flat tails of some of these curves at low SFR suggest that even the $60m_{\text{SPH}}$ criterion may be a bit too loose. Although we compute each galaxy’s “instantaneous” SFR using equation (1), we find that the SFR is reasonably steady over timescales of 200

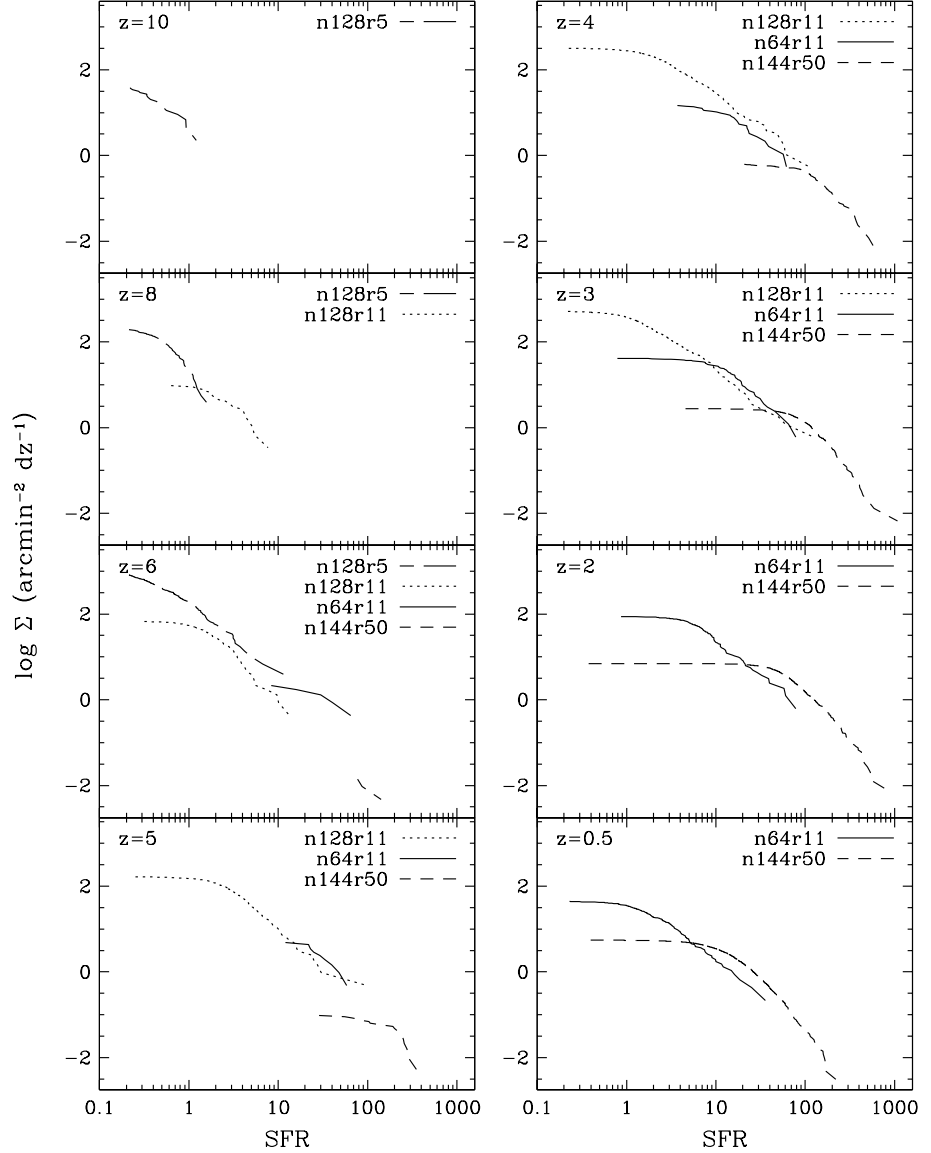


Figure 1. The cumulative distribution of galaxies as a function of instantaneous star formation rate, from $z = 10$ to $z = 0.5$, in simulations of the LCDM model with different numerical parameters. Each curve shows the surface density of simulated galaxies, in number per arcmin² per unit redshift, with star formation rate above the value indicated on the x -axis. Legends indicate the simulation box size (5.55, 11.11, or $50h^{-1}$ Mpc) and particle number (64^3 , 128^3 , or 144^3 particles of each species).

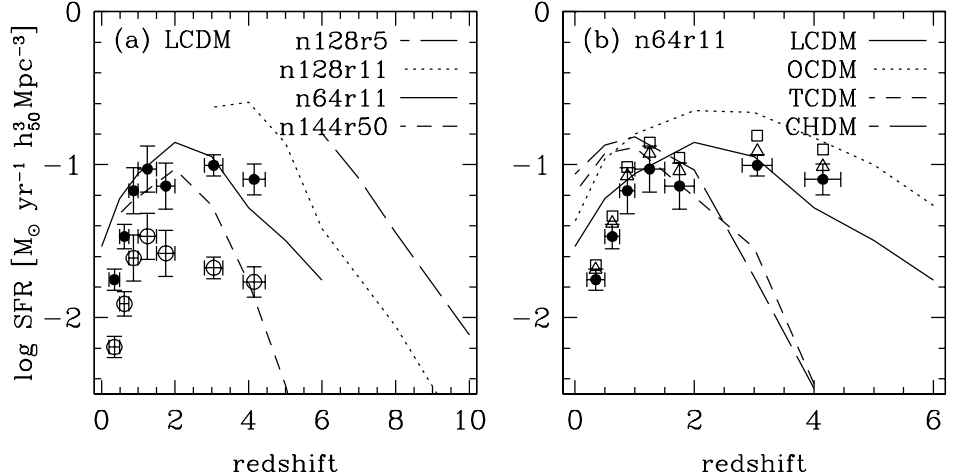


Figure 2. Globally averaged star formation rates as a function of redshift in (a) simulations of the LCDM model with various numerical parameters, and (b) simulations of various CDM models, all with 64^3 particles in an $11.11h^{-1}$ Mpc box. Note the different ranges of the x -axis in the two panels. Data points are taken from the compilation by Steidel et al. (1999). In (a), filled and open circles show estimates with and without extinction corrections, corrected to the LCDM cosmological parameters. In (b), extinction-corrected estimates are shown for the cosmological parameters of LCDM (filled circles), OCDM (open triangles), and TCDM/CHDM (open squares).

Myr, and our results would therefore not be very different if we averaged over time intervals up to this value.

Figure 2a shows the average comoving density of star formation as a function of redshift, a representation made famous by Madau et al. (1996), for the same simulations plotted in Figure 1. Of course, a given simulation only includes the contribution of galaxies above the resolution limit listed in Table 1. At any given redshift, the higher resolution simulation always has a higher comoving density of star formation, and the difference between simulations generally grows with increasing redshift because the contribution of low mass galaxies is more important at higher z . Thus, the highest line at a given redshift in Figure 2a should be taken as a lower limit to the predicted SFR. It is tempting to draw an envelope that connects the tops of the long-dashed, dotted, and solid curves, but it is not clear that even this combined result is numerically converged, especially at $z > 5$.

The data points in Figure 2a, kindly provided by C. Steidel, are taken from the compilation by Steidel et al. (1999), based on their own data ($z > 3$) and the data of Lilly et al. (1996, $z < 1$) and Connolly et al. (1997; $1 < z < 2$). Filled circles include Steidel et al.'s estimated corrections for extinction of the rest-frame UV continuum, a factor of 2.75 at $z < 2$ and 4.68 at $z > 2$. Open circles have no extinction correction. We have converted all values to our $\Omega_m = 0.4$, $\Omega_\Lambda = 0.6$ cosmology.

Given that higher numerical resolution should only increase the predicted SFR, it appears that the LCDM simulations predict more star formation than is inferred from UV continuum observations, at least with Steidel et al.’s (1999) extinction estimates. Given the uncertainties in the observational estimates (which depend on assumed IMF shapes and population synthesis models in addition to extinction corrections), it is premature to draw strong conclusions from this comparison. However, the impression of excessive star formation is also supported by an independent comparison at $z = 0$. The n64r11 simulation predicts a density parameter $\Omega_\star = 0.0146$ in stars at $z = 0$. This is roughly four times higher than Fukugita et al.’s (1998) observational estimate, $\Omega_\star = 0.0038^{+0.0024}_{-0.0017}$. If the simulations are to reproduce observational estimates of Ω_\star at $z = 0$, then a large fraction of the gas that is cooling into galaxies must actually be forming baryonic dark matter rather than luminous stars. Katz et al. (1992) reached a similar conclusion for an $\Omega_m = 1$ CDM model, and Pearce et al. (1999) reached a similar conclusion for LCDM with an independent simulation.

Figure 2b shows global star formation rates for the four CDM simulations analyzed in Davé et al.’s (1998) study of the low-redshift Ly α forest: a flat model with a cosmological constant (LCDM), an open universe model with $\Omega_m = 0.5$ (OCDM), and two $\Omega_m = 1$ models, one with a tilted inflationary spectrum ($n = 0.8$, TCDM), and one with a hot dark matter component ($\Omega_\nu = 0.2$, CHDM). All of these simulations use 64^3 particles of each species in an $11.11h^{-1}$ Mpc box; the LCDM simulation is the same as the one labeled n64r11 in Figures 1 and 2a. The differences in predicted star formation histories clearly reflect the differences in the overall history of mass clustering in the various models. The open model has the earliest structure formation, and its star formation history peaks at the highest redshift and shows the most rapid decline between $z = 1$ and $z = 0$. The $\Omega_m = 1$ models, on the other hand, form structure relatively late, and their global star formation rates decline only mildly at low redshift. Because of their low mass fluctuation amplitudes and relatively late structure formation, the TCDM and CHDM models appear to be in serious conflict with the observationally estimated star formation rates at $z > 3$. However, this conclusion could be sensitive to the finite numerical resolution of the simulations, since the main contribution to the global SFR in these models will come from galaxies below our resolution limit.

One of the striking features of the observed Lyman-break galaxy (LBG) population is its high clustering amplitude, similar to that of bright galaxies at $z = 0$ (Adelberger et al. 1998; Giavalisco et al. 1998; Steidel et al. 1998). This strong clustering has a straightforward theoretical explanation, analogous to the one given by Kaiser (1984) for the strong clustering of Abell clusters at $z = 0$. Like clusters today, LBGs are “rare” objects relative to the scale of non-linear mass clustering (at $z = 3$), and as a result they are highly biased tracers of the underlying mass distribution. Numerical or analytic models that associate observed LBGs with massive dark halos can therefore explain their observed clustering amplitude without much difficulty.

KHW found that the clustering of high redshift galaxies was remarkably insensitive to the adopted cosmological model, because differences in bias mask differences in clustering of the underlying mass distributions. Analytic models lead to a similar conclusion (e.g., Adelberger et al. 1998). The small volume

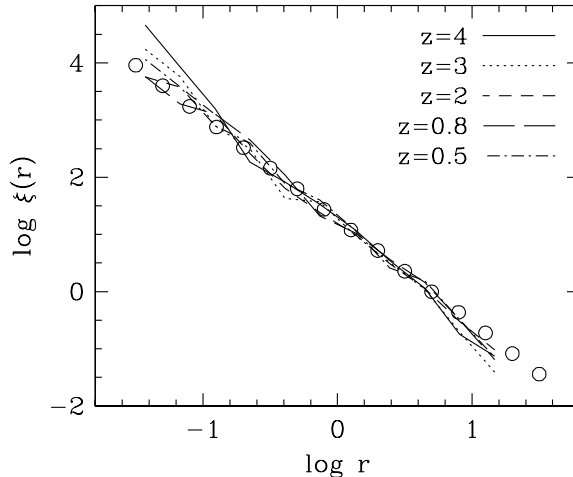


Figure 3. Galaxy correlation functions in the LCDM model as a function of redshift, with r in comoving h^{-1} Mpc, from the n144r50 simulation. At each redshift, the correlation function is measured for the 365 most massive galaxies in the box. Open circles show a power-law, $\xi(r) = (r/5h^{-1} \text{ Mpc})^{-1.8}$.

of the KHW simulations ($11.11h^{-1}$ Mpc cubes) made a direct comparison to existing spectroscopic samples of LBGs difficult, so in Figure 3 we show results for the LCDM model from our n144r50 simulation. At each redshift we select the 365 most massive galaxies (which is the full population at $z = 4$ and a decreasing fraction at lower z), so that we measure the clustering of a sample of fixed comoving space density, $n = 0.0029 h^3 \text{ Mpc}^{-3}$ (0.2 galaxies per arcmin² per unit redshift at $z = 3$). Although the dark matter clustering grows steadily from $z = 4$ to $z = 0.5$, the galaxy correlation function stays virtually constant, well described at all redshifts by a power law $\xi(r) = (r/5h^{-1} \text{ Mpc})^{-1.8}$. This result agrees well with that of Pearce et al. (1999), who use a similar numerical technique. Cen & Ostriker (1999), using a very different numerical technique, find nearly identical values for the comoving correlation length but a steeper correlation function slope.

3. Some Outstanding Issues

Hydrodynamic simulations of models like LCDM seem to provide a fairly good account of galaxy formation. Standard gas dynamics and radiative cooling combined with plausible recipes for star formation lead to objects with roughly the right sizes and masses to represent the luminous regions of observed galaxies. Simulations easily reproduce the observed abundance of Lyman-break galaxies, and the global star formation history that they predict has at least roughly the shape suggested by observations. The simulated galaxy populations also exhibit approximately the correct clustering strength at $z = 0$ and at $z = 3$. Semi-analytic models can claim similar successes (e.g., Baugh et al. 1998, Governato et al. 1998, Benson et al. 1999, Kauffmann et al. 1999ab, Somerville et al. 1999),

though it is not yet clear whether the agreement of end results between the two approaches arises (as one would hope) because both are correctly modeling the same underlying physics. Indeed, two semi-analytic models that adopt quite different scenarios for the nature of Lyman-break galaxies can both reproduce their observed properties fairly well (Baugh et al. 1998, Somerville et al. 1999).

An optimist would certainly conclude that the glass containing our current theoretical understanding of galaxy formation is at least half full. However, there are some nagging discrepancies that should not escape mention, since they may well turn out to have interesting implications. First is the problem already mentioned in §2, a tendency for hydrodynamic simulations to process too many baryons into stars. Baryonic dark matter is an acceptable solution to this problem, but it is discomfoting to be forced into such a dodge. A second difficulty arises in simulations of individual galaxies: lumpy, dissipative collapse causes baryons to transfer angular momentum to the dark matter halo, with the result that the final galaxy disks are too small (Navarro & White 1994, Navarro & Steinmetz 1997). The third and fourth problems appear in high-resolution, collisionless N-body simulations (no gas dynamics), which predict dark matter halos that are too concentrated to match observed rotation curves (Moore 1994, Flores & Primack 1994, Moore et al. 1999b, Navarro & Steinmetz 1999, but see Kravtsov et al. 1998), and an abundance of low mass satellite galaxies far in excess of the number observed in the Local Group (Klypin et al. 1999, Moore et al. 1999a).

Each of these apparent discrepancies rests on a handful of technically challenging numerical simulations, and one or more of them might fade as the simulations (or the observational data) improve. However, it seems likely that at least some of these are genuine physical problems. The solutions may lie in the astrophysics of galactic scale star formation — in particular, strong supernova feedback is often invoked as a way to reduce the overall level of star formation, delay gas cooling so as to suppress angular momentum loss, prevent star formation in low mass satellite halos, and perhaps even rearrange the mass in galaxy cores enough to change rotation curve shapes (Navarro et al. 1996). Alternatively, the solutions may require changes to the fundamental tenets of the cosmological models, such as the spectrum of primordial fluctuations or the assumption that dark matter is cold and non-interacting. There is enough commonality to the problems to suggest that they may well have a common set of solutions. Comparison between increasingly accurate theoretical calculations and the growing web of observational constraints at all redshifts should eventually tell us whether those solutions lie in gas dynamics, star formation, early universe physics, or the nature of dark matter.

References

- Adelberger, K. L., Steidel, C. C., Giavalisco, M., Dickinson, M., Pettini, M., & Kellogg, M. 1998, *ApJ*, 505, 18
Anninos, P., & Norman, M. L. 1996, *ApJ*, 459, 12
Avila-Reese, V., Firmani, C., & Hernandez, X. 1998, *ApJ*, 505, 37
Barnes, J.E., & Hut, P. 1986, *Nature*, 324, 446

- Baugh, C. M., Cole, S., Frenk, C. S., & Lacey, C. G. 1998, *ApJ*, 498, 504
- Benson, A. J., Cole, S., Frenk, C. S., Baugh, C. M., & Lacey, C. G. 1999, *MNRAS*, submitted, astro-ph/9903343
- Bond, J. R., Cole, S., Efstathiou, G., & Kaiser, N. 1991, *ApJ*, 379, 440
- Bower, R. 1991, *MNRAS*, 248, 332
- Cen, R., & Ostriker, J. P. 1992, *ApJ*, 399, L113
- Cen, R., & Ostriker, J. P. 1999, *ApJ*, submitted, astro-ph/9809370
- Cole, S., Aragon-Salamanca, A., Frenk, C. S., Navarro, J. F., & Zepf, S. E. 1994, *MNRAS*, 271, 781
- Connolly, A. J., Szalay, A. S., Dickinson, M., SubbaRao, M. U., & Brunner, R. J. 1997, *ApJ*, 486, L11
- Dalcanton, J. J., Spergel, D. N., & Summers, F. J. 1997, *ApJ*, 482, 659
- Davé, R., Dubinski, J., & Hernquist, L. 1997, *New Astron*, 2, 227
- Davé, R., Hernquist, L., Katz, N., & Weinberg, D. H. 1998, *ApJ*, 511, 521
- Domínguez-Tenreiro, R., Tissera, P. B., & Sáiz, A. 1998, *ApJ*, 508, L123
- Evrard, A.E., Summers, F.J., & Davis, M. 1994, *ApJ*, 422, 11
- Fall, S. M., & Efstathiou, G. 1980, *MNRAS*, 193, 189
- Flores, R. A., & Primack, J. R. 1994, *ApJ*, 427, L1
- Fukugita, M., Hogan, C. J., & Peebles, P. J. E. 1998, *ApJ*, 503, 518
- Giavalisco, M., Steidel, C.C., Adelberger, K.L., Dickinson, M.E., Pettini, M. & Kellogg, M. 1998, *ApJ*, 503, 543
- Gnedin, N. 1995, *ApJS*, 97, 231
- Governato, F., Baugh, C.M., Frenk, C.S., Cole, S., Lacey, C.G., Quinn, T.R. & Stadel, J. 1998, *Nature*, 392, 359
- Hernquist, L., & Katz, N. 1989, *ApJS*, 70, 419
- Kaellander, D., & Hultman, J. 1998, *A&A*, 333, 399
- Kaiser, N. 1984, *ApJ*, 294, L9
- Katz, N. 1992, *ApJ*, 391, 502
- Katz, N., & Gunn, J. E. 1991, *ApJ*, 377, 365
- Katz, N., Hernquist, L., & Weinberg, D. H. 1992, *ApJ*, 399, L109
- Katz, N., Hernquist, L., & Weinberg, D. H. 1999, *ApJ*, in press, astro-ph/9806257 (KHW)
- Katz, N., Weinberg D.H., & Hernquist, L. 1996, *ApJS*, 105, 19
- Kauffmann, G., Colberg, J. M., Diaferio, A., & White, S. D. M. 1999a, *MNRAS*, 303, 188
- Kauffmann, G., Colberg, J. M., Diaferio, A., & White, S. D. M. 1999b, *MNRAS*, submitted, astro-ph/9809168
- Kauffmann, G., White, S. D. M., & Guideroni, B. 1993, *MNRAS*, 264, 201
- Klypin, A. A., Kravtsov, A. V., Valenzuela, O., & Prada, F. 1999, *ApJ*, submitted, astro-ph/9901240
- Kravtsov, A. V., Klypin, A. A., Bullock, J. S., & Primack, J. R. 1998, *ApJ*, 502, 48

- Lacey, C., & Cole, S. 1994, MNRAS, 271, 676
- Lilly, S. J., LeFevre, O., Hammer, F., & Crampton, D. 1996, ApJ, 460, L1
- Madau, P., Ferguson, H. C., Dickinson, M. E., Giavalisco, M., Steidel, C. C., & Fruchter, A. 1996, MNRAS, 283, 1388
- Mo, H. J., Mao, S., & White, S. D. M. 1998, MNRAS, 295, 319
- Moore, B. 1994, Nature, 370, 629
- Moore, B., Ghigna, S., Governato, F., Lake, G., Quinn, T., Stadel, J., & Tozzi, P. 1999a, ApJ, submitted, astro-ph/9907411
- Moore, B., Quinn, T., Governato, F., Stadel, J., & Lake, G. 1999b, MNRAS, submitted, astro-ph/9903164
- Navarro, J. F., Eke, V. R., & Frenk, C. S. 1996, MNRAS, 283, L72
- Navarro, J. F., & Steinmetz, M. 1997, ApJ, 478, 13
- Navarro, J. F., & Steinmetz, M. 1999, ApJ, in press, astro-ph/9908114
- Navarro, J., & White, S. D. M. 1994, MNRAS, 267, 401
- Pearce, F. R., Jenkins, A., Frenk, C. S., Colberg, J. M., White, S. D. M., Thomas, P. A., Couchman, H. M. P., Peacock, J. A., & Efstathiou, G. 1999, ApJ, in press, astro-ph/9905160
- Pen, U. 1998, ApJS, 115, 19
- Press, W. H., & Schechter, P. 1974, ApJ, 187, 425
- Somerville, R. S., & Primack, J. R. 1999, MNRAS, in press, astro-ph/9802268
- Somerville, R. S., Primack, J. R., & Faber, S. M. 1998, MNRAS, submitted, astro-ph/9806228
- Steidel, C., Adelberger, K., Dickinson, M., Giavalisco, M., Pettini, M., Kellogg, M. 1998, ApJ, 492, 428
- Steidel, C., Adelberger, K., Giavalisco, M., Dickinson, M., & Pettini, M. 1999, ApJ, 519, 1
- Steidel, C. C., Giavalisco, M., Pettini, M., Dickinson, M., & Adelberger, K. L. 1996, ApJ, 462, L17
- Steinmetz, M., & Müller, E. 1994, A&A, 281, L97
- Vedel, H., Hellsten, U., & Sommer-Larsen, J. 1994, MNRAS, 271, 743
- White, S. D. M., & Frenk, C. S. 1991, ApJ, 379, 52
- White, S. D. M., & Rees, M. J. 1978, MNRAS, 183, 341